AAPS PharmSciTech, Vol. 13, No. 4, December 2012 (© 2012)
DOI: 10.1208/s12249-012-9868-2

Research Article

Solid Dispersion of Ursolic Acid in Gelucire 50/13: a Strategy to Enhance Drug Release and Trypanocidal Activity

Josimar de Oliveira Eloy,[1] Juliana Saraiva,[1] Sergio de Albuquerque,[1] and Juliana Maldonado Marchetti[1,2]

Received 15 December 2011; accepted 27 September 2012; published online 16 October 2012

Abstract. Solid dispersions (SDs) are an approach to increasing the water solubility and bioavailability of lipophilic drugs such as ursolic acid (UA), a triterpenoid with trypanocidal activity. In this work, Gelucire 50/13, a surfactant compound with permeability-enhancing properties, and silicon dioxide, a drying adjuvant, were employed to produce SDs with UA. SDs and physical mixtures (PMs) in different drug/carrier ratios were characterized and compared using differential scanning calorimetry, hot stage microscopy, Fourier transform infrared spectroscopy (FTIR), X-ray diffraction (XRD), particle size, water solubility values, and dissolution profiles. Moreover, LLC-MK2 fibroblast cytotoxicity and trypanocidal activity evaluation were performed to determine the potential of SD as a strategy to improve UA efficacy against Chagas disease. The results demonstrated the conversion of UA from the crystalline to the amorphous state through XRD. FTIR experiments provided evidence of intermolecular interactions among the drug and carriers through carbonyl peak broadening in the SDs. These findings helped explain the enhancement of water solubility from 75.98 μg/mL in PMs to 293.43 μg/mL in SDs and the faster drug release into aqueous media compared with pure UA or PMs, which was maintained after 6 months at room temperature. Importantly, improved SD dissolution was accompanied by higher UA activity against trypomastigote forms of *Trypanosoma cruzi*, but not against mammalian fibroblasts, enhancing the potential of UA for Chagas disease treatment.

KEY WORDS: Chagas disease; Gelucire 50/13; solid dispersions; solvent evaporation method; ursolic acid.

INTRODUCTION

Many potential drug candidates never reach the market because of low bioavailability, which can be a consequence of low solubility or limited gastrointestinal tract permeability. Methods for overcoming this problem include size reduction, surfactant use, salt formation, pH adjustment, cyclodextrin complex formation, pro-drug formulations, and liposome preparation (1). Among commonly utilized methods, one of the most efficacious is the use of solid dispersions (SDs), which are defined as molecular or amorphous drug mixtures with low water solubility and hydrophilic carriers that improve the drug dissolution profile (2,3).

These enhanced dissolution profiles are attributed to particle size reduction, reduced agglomeration, improved wettability, and drug conversion from a crystalline structure to a more soluble, amorphous form (4). The use of a hydrophilic polymer enhances drug dissolution, which makes its selection critical for developing a successful solid dispersion. Polyethylene glycols and polyvinylpyrrolidones are among the polymers that are most frequently employed as carriers in solid dispersions, but polymers with inherent surfactant properties improve the dissolution properties of many lipophilic drugs. This class of solid dispersion polymers also has the advantage of avoiding drug recrystallization, a stability problem that is commonly associated with solid dispersions. Recrystallization can be prevented with use of surfactants such as Poloxamers and Gelucires, which reportedly enhance oral bioavailability *in vivo* (5,6). Gelucires belong to a family of vehicles that are derived from mixtures of mono-, di-, and triglycerides and polyethylene glycol fatty acid esters. Gelucires with different properties are available, including various HLB values (1–18) and melting points (33–70°C) (5). They have successfully been used as carriers in solid dispersions of indomethacin (7), nifedipine (8), glibenclamide (9), and diclofenac (10). Gelucire enhances biological membrane penetration and could thus increase the bioavailability of drugs displaying low oral absorption (11).

In this work, solid dispersions with Gelucire 50/13 and silicon dioxide, a drying adjuvant, have been generated as an approach to enhance the lipophilic molecule ursolic acid (UA) dissolution profile, for which low bioavailability limits its therapeutic potential (12). Ursolic acid is a pentacyclic triterpenoid (13) that possesses anti-inflammatory (14), anti-cancer (15), hepatoprotective (16), and trypanocidal (17) pharmacological properties. Among these, the trypanocidal activity is of particular interest to our research group because we want to

[1] Faculty of Pharmaceutical Sciences of Ribeirão Preto, University of São Paulo, Ribeirão Preto, Avenida do Café s/n, 14040-903 Ribeirão Preto, São Paulo, Brazil.
[2] To whom correspondence should be addressed. (e-mail: jmarchet@usp.br)

improve Chagas disease treatment. Chagas disease is caused by *Trypanosoma cruzi* and is a life-threatening pathology affecting approximately 15 million people, mostly in Latin America. The current treatment, 2-nitroimidazole benznidazole (Rochagan®), displays limited efficacy in the chronic disease phase of Chagas and is toxic to patients. Therefore, other drugs must be investigated that are more efficient and less toxic (18). Our group has previously developed solid dispersions employing polyethylene glycol 6000 and Poloxamer 407 as carriers; however, despite an improvement in the ursolic acid dissolution profile in Poloxamer 407-prepared products, the *in vitro* trypanocidal activity was not enhanced, which could be attributed to low drug penetration in the parasite cell. Therefore, we studied the lipid carrier Gelucire 50/13 in solid dispersion preparation (Fig. 1).

Solid dispersions and physical mixtures (PMs) in different drug and carrier ratios were characterized and compared using differential scanning calorimetry (DSC), hot stage microscopy (HSM), Fourier transform infrared spectroscopy (FTIR), X-ray diffraction (XRD), particle size, water solubility values, and dissolution profiles. Moreover, cytotoxicity against LLC-MK2 fibroblasts and trypanocidal activity were evaluated to determine the potential of solid dispersion to improve ursolic acid efficacy against Chagas disease.

MATERIALS AND METHODS

Materials

UA was purchased from Idealfarma (Brazil); high-performance liquid chromatography (HPLC) grade acetonitrile and methanol were purchased from Merck (Germany). Gelucire 50/13 was a kind gift from Gattefossé (France).

Methods

Solid Dispersion and Physical Mixture Preparation

Solid dispersions containing the drug, Gelucire, and silicon dioxide in ratios of 1:0.6:0.4 (SD 001), 1:3:1 (SD002), 1:7:2 (SD003), and 1:15:4 (SD004) (*w*/*w*/*w*) were prepared by the solvent method. The drug and carriers were dissolved in methanol (10% *w*/*v*), and the solvent was subsequently evaporated at room temperature while stirring. The products were then stored in an oven at 40°C for 24 h to ensure complete methanol evaporation, followed by pulverization with a mortar and pestle. The PMs were prepared by grinding the drug and carriers together using a mortar and pestle.

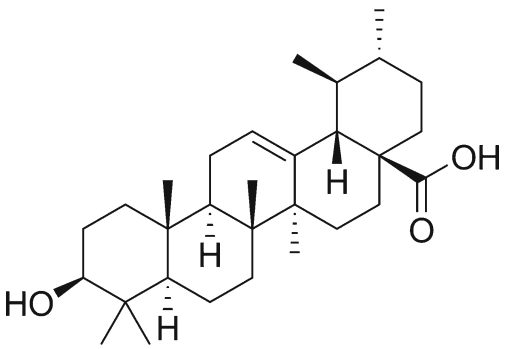

Fig. 1. Chemical structure of ursolic acid

Solid Dispersion and Physical Mixture Characterization

Fourier Transform Infrared Spectroscopy

FTIR analyses were conducted using a Shimadzu IRPrestige-21 instrument. The samples were previously ground and mixed thoroughly with potassium bromide. The potassium bromide disks were prepared by compressing the powders in a hydraulic press. Scans were obtained at a resolution of 2 cm^{-1} from 4,000 to 400 cm^{-1} (Fig. 2).

Differential Scanning Calorimetry

DSC measurements were performed using a Shimadzu DSC-50 instrument. Samples were placed in aluminum pans and heated from 30°C to 330°C at a rate of 10°C/min. Calibration was performed using indium and *n*-octadecane as reference materials.

Hot Stage Microscopy

Sample HSM was conducted with a TMSSG 600 (Linkam) instrument assembled on an Axioplan 2 Image (Zeiss) microscope equipped with an Axiocam HRC camera (Zeiss). A small amount (2–4 mg) of sample was placed on a glass slide with a cover slip and heated at a rate of 10°C/min. Changes in sample morphology were photographed.

X-ray Diffraction

X-ray diffraction measurements were performed using a Siemens/D5005 instrument with a copper anode operating under CuK radiation (1.5406 Å, 40 kV, and 30 mA). Patterns were obtained using a step width of 0.05°/s from 2° to 50° at room temperature on a 2Θ scale.

Drug Content Determination

The amount of UA in the PMs and SDs was determined by HPLC, following a method previously developed and validated by our group (19). The equipment used was a Shimadzu HPLC equipped with an LC-10ADVP pump, a SPD-10A VP UV detector, and a model CR6-A integrator. The analyte was eluted with a mobile phase composed of acetonitrile/water (88:12, *v*/*v*) at a 1.0-mL/min flow rate using a 20-μL total injection volume. UV detection was performed at 203 nm, and separation was accomplished using a C18 reverse-phase column (LiChrospher® (Merck), 250×4 mm (5 μm)) at room temperature (25°C). To analyze UA content, SD and PM samples containing 2.5 mg UA were dissolved in 100 mL acetonitrile and filtered through a 0.45-μm membrane before HPLC analysis (n=3).

Particle Size

Particle size was measured with a Beckman Coulter LS 13 320 laser diffraction particle size analyzer.

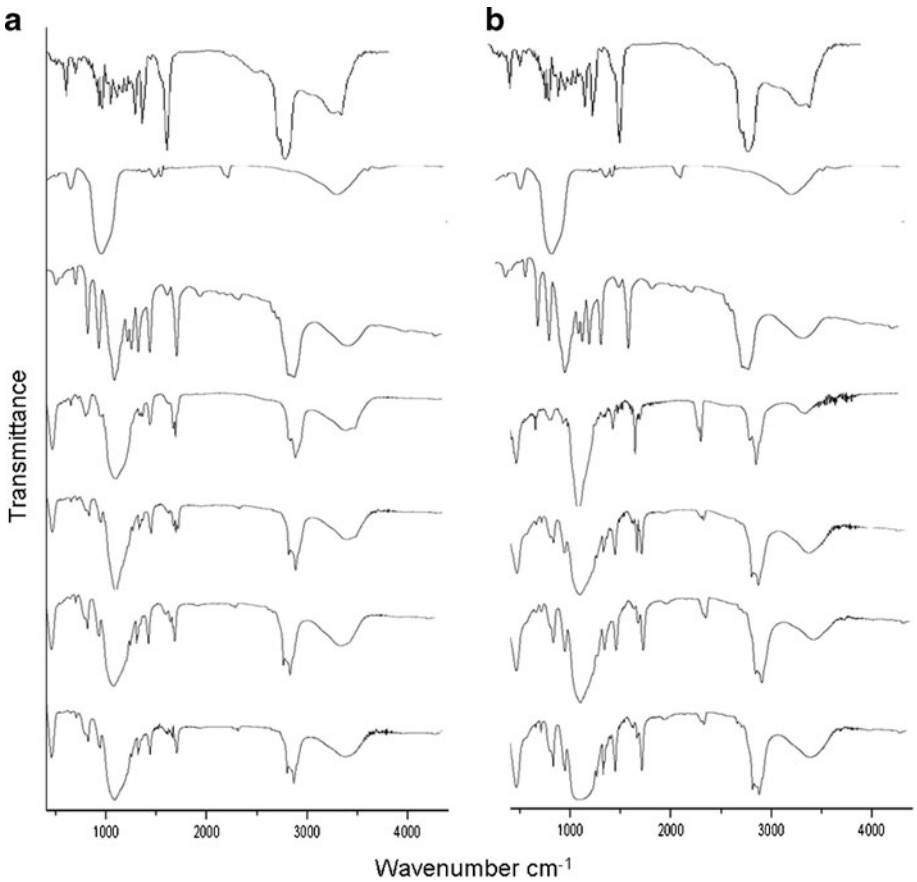

Fig. 2. FTIR analyses of UA, silicon dioxide, Gelucire, SDs (**a**), and PMs (**b**) containing 50%, 80%, 90%, and 95% (*w*/*w*) of the carrier, from *top* to *bottom*

Solid Dispersion and Physical Mixture Evaluation

Water Solubility

Pure UA, PM, or SD solubility in water was measured by adding the drug in excess (10 mg) to 10 mL distilled water with magnetic stirring (300 rpm) at 25°C for 24 h. Samples were filtered (0.45 μm), dissolved in acetonitrile (1:10, *w*/*v*), and analyzed by HPLC (n=3).

Dissolution Profile

Dissolution studies were conducted on an SR8 Plus Hanson Corporation instrument (Chatsworth, CA, USA). A sample amount equivalent to 7.5 mg UA was added to 900 mL phosphate buffer at pH 6.8 containing 1% sodium lauryl sulfate (37°C±0.2°C), and the mixture was stirred with a paddle at 75 rpm. At predetermined times, 1-mL aliquots were withdrawn, replaced by fresh media, and filtered (0.45 μm) before dilution (1:10, *v*/*v*) and HPLC analysis.

Cytotoxicity

SD and PM containing 5% drug were evaluated for cytotoxicity on LLC-MK2 fibroblasts with the MTT method (20). Briefly, LLCMK2 cells (1×10^6/mL) were cultured in 96-well plates containing products at the following dilutions: 8, 32, 128, 256, and 500 μM. Plates were incubated in a CO_2 incubator at 5% CO_2 and 37°C for 24 h. Ten-microliter MTT solution (5 mg/mL) was then added to each well, and plates were incubated for 4 h. Then, 100 μL of acid isopropyl was added, followed by room temperature incubation for 1 h. The plate was read on a spectrophotometer at 595 nm.

Trypanocidal Bioassay

SD and PM containing 5% drug were evaluated for trypanocidal activity using infected blood according to a method described by Grael and collaborators (21). Briefly, Swiss albino mice that had been infected with the *T. cruzi* 'Y' strain were used to provide trypomastigote forms. Infected blood was collected at the parasitemic peak (7 days after infection; 1×10^6 parasites/mL) through cardiac puncture using heparin as an anticoagulant in a 7:3 blood/anticoagulant ratio. The assays were performed in 96-well microplates; aliquots of the PM004 and SD004 products were added to the diluted blood to give final concentrations of 8, 32, 128, and 256 μM. The microplates were kept stirring at 4°C for 24 h, and parasite number was determined according to Brener (22). All of the bioassays were performed in triplicate. The results are presented as the lysis percentages of *T. cruzi* trypomastigote forms, representing trypanocidal activity. The inhibitory concentration (IC_{50}) was calculated with a sigmoidal dose–response curve.

RESULTS

Solid Dispersion and Physical Mixture Characterization

Fourier Transform Infrared Spectroscopy

UA has characteristic bands that should be highlighted. The band at approximately 1,650 cm^{-1} corresponds to the UA carbonyl group, and the band at approximately 3,400 cm^{-1} was attributed to the UA hydroxyl group. Carbonyl and hydroxyl groups are also present in the Gelucire chemical structure, and the corresponding bands were observed in its spectrum. Silicon dioxide exhibits two characteristic bands, one at approximately 1,000 cm^{-1}, which is attributed to a S=O stretching vibration, and another at approximately 3,400 cm^{-1}, which is associated with O-H stretching vibrations of water molecules adhered to its highly hydrophilic surface. The PM and SD spectra contained carrier and drug in different proportions and exhibited all of the previously mentioned bands, confirming the presence of drug and carriers in the products. The carbonyl groups appeared as sharp bands in the PMs and were less intense in the SDs.

Differential Scanning Calorimetry

As observed in Fig. 3, the DSC curve of pure UA has an exothermic peak at approximately 200°C, which is related to a crystallization event, and an endothermic peak at approximately 280°C, which is related to a melting process. Gelucire shows a broad endotherm at approximately 45°C, which is also related to its melting, whereas silicon dioxide does not present an endotherm because of its high melting temperature. In the PM DSC curves, the Gelucire endotherm peak is observable for all formulations, but the UA peak can only be identified in the PMs containing 50% or 20% drug. SD curves containing 50% UA attributed the peak to the drug but not the Gelucire endotherm. The product containing 20% drug exhibited peaks for both the carrier and the drug, but the UA peak was reduced. The SDs prepared with 5% and 10% drug had DSC curves that were identical to the PMs, in which only the peak corresponding to Gelucire was present.

Hot Stage Microscopy

The HSM observation in Fig. 4 shows a thermal event at approximately 200°C for UA, both as the pure drug and in the PM, in which small needle-like crystals appear before melting completely. This phenomenon is not observed in Gelucire, which melts at approximately 45°C, nor is it observed in the SD containing 95% carrier.

X-ray Diffraction

The UA diffraction pattern in Fig. 5 reveals three characteristic peaks at 6°, 8°, and 15°. Gelucire had two apparent peaks at 19° and 23°. The other carrier, silicon dioxide, did not exhibit any diffraction peaks in the range examined. The PMs diffraction patterns contain peaks corresponding to both UA and Gelucire that are proportional to their concentrations in

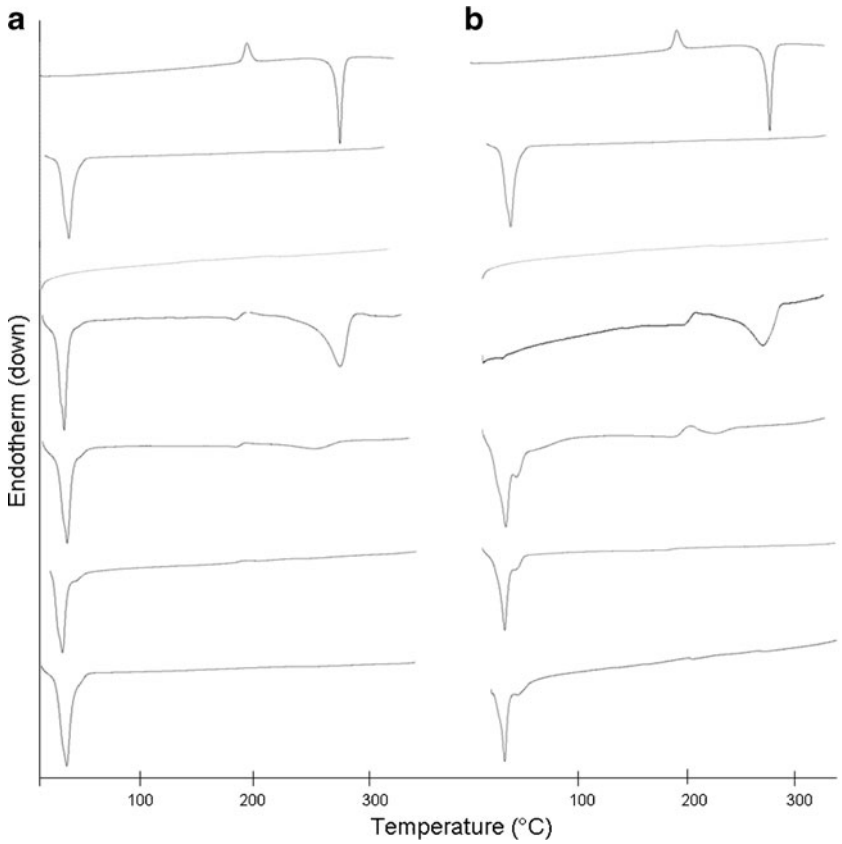

Fig. 3. DSC analyses of UA, silicon dioxide, Gelucire, PMs (**a**), and SDs (**b**) containing 50%, 80%, 90%, and 95% (w/w) of the carrier, from *top* to *bottom*

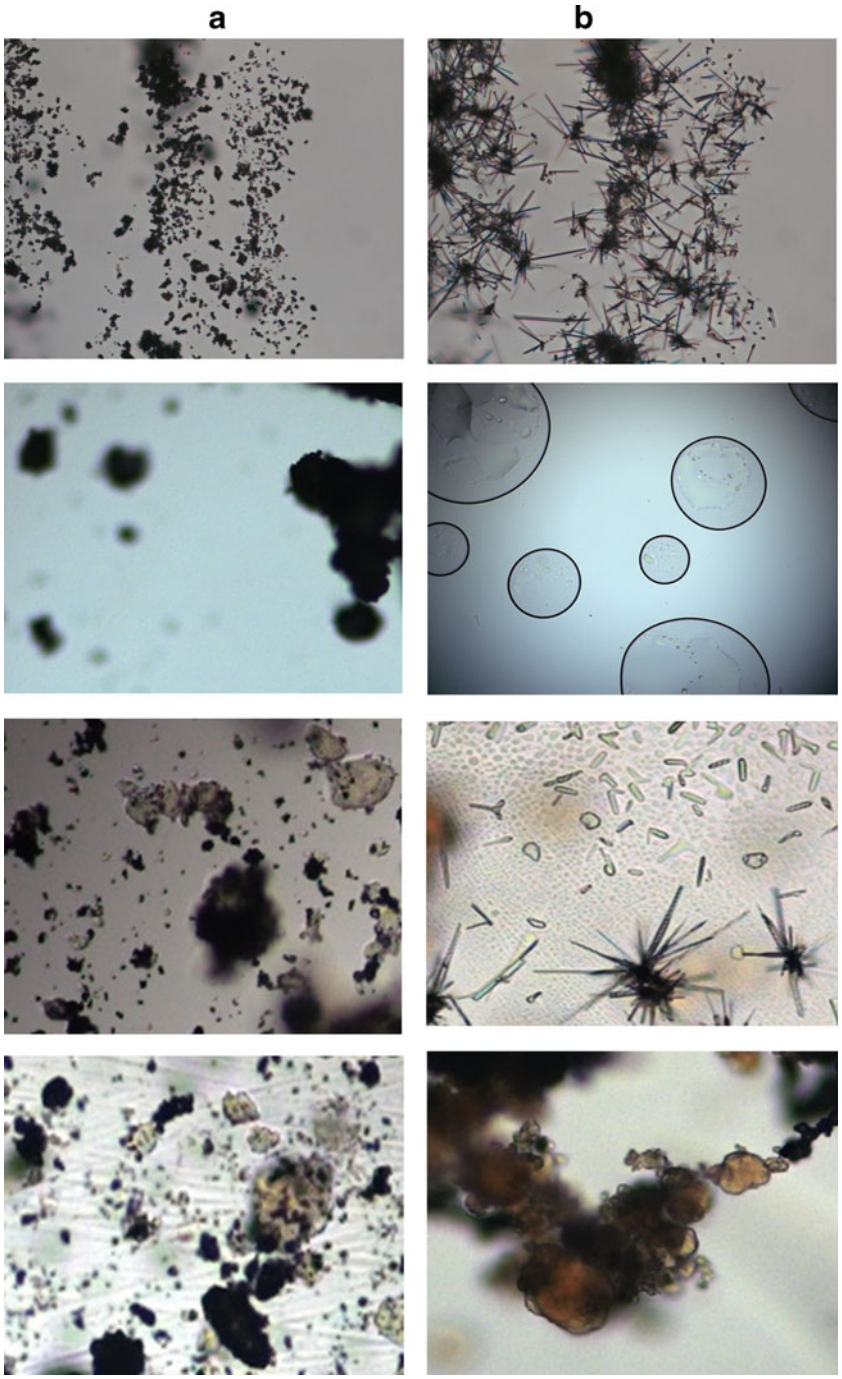

Fig. 4. HSM photomicrographs at 25°C (**a**) and 200°C (**b**) of UA, Gelucire, PM, and SD containing 95% (*w*/*w*) of the carrier, from *top* to *bottom*

the mixture. The pattern was different for the SDs. In the SDs containing 50% drug, peaks attributed to the drug at 8° and 15° can be identified, but they are broadened compared with the pure drug or with the PM. Additionally, the Gelucire X-ray peaks disappeared. The Gelucire peaks were present for the other SDs, whereas the UA peaks are progressively smaller and almost disappear in the product containing 5% drug. PMs containing 5% UA displayed peaks corresponding to the drug after storage at room temperature after 6 months, whereas the same peaks were not present in SDs containing the same drug load.

Drug Content Determination

Results in Table I show UA content as a percentage of the total amount added to the PMs and SDs, which ranged from 88.79% for PM002 to 109.33% for PM001.

Particle Size

Table II shows the results of UA particle size, SDs, and PMs in different drug/carrier ratios. The values ranged from 59.38 μm for SD004, which was prepared with 5% UA, to

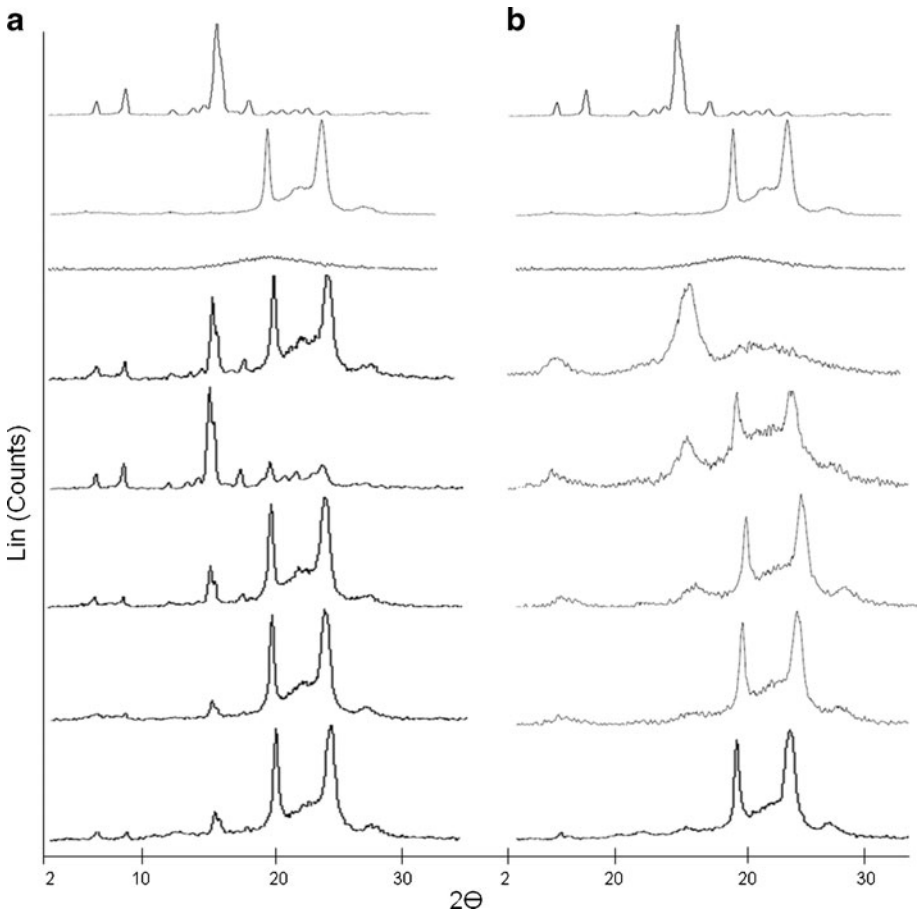

Fig. 5. X-ray analyses of UA, silicon dioxide, Gelucire, PMs (**a**), and SDs (**b**) containing 50%, 80%, 90%, 95%, and 95% (*w*/*w*) after 6 months at room temperature of the carrier, from *top* to *bottom*

115.70 μm for SD001, which was prepared with 50% UA (Fig. 6).

Solid Dispersions and Physical Mixture Evaluation

Water Solubility

The UA solubility values in PMs and SDs for different carrier to drug ratios are shown in Fig. 7. UA solubility is increased in systems containing higher percentages of the carrier. The average UA solubility values in micrograms per milliliter are 2.12, 11.49, 22.62, and 75.98 for PMs containing 50%, 80%, 90%, and 95% of the carrier, respectively, and 5.49, 26.08, 79.97, and 293.43 for SDs containing 50%, 80%, 90%, and 95% of the carrier, respectively.

Drug Release

The UA dissolution profile as a pure drug in PMs and in SDs for different drug/carrier loads are represented in Fig. 7. When dissolved in phosphate-buffered medium containing 1% sodium lauryl sulfate, pure UA has a dissolution profile similar to that of its PMs; after 4 h, approximately 15% of the drug is dissolved. However, the SDs dissolved faster compared

Table I. UA Content Determination (in Percent) of the Amount Labeled in PMs and SDs in Different Drug/Carrier Loads

Product	UA content (%)
PM001	109.33±3.51
PM002	88.79±2.58
PM003	90.25±1.25
PM004	95.98±1.56
SD001	89.79±3.28
SD002	90.18±4.85
SD003	104.56±3.96
SD004	91.16±0.97
PM004 after 6 months	93.85±2.47
SD004 after 6 months	90.03±3.02

UA ursolic acid, *PM* physical mixture, *SD* solid dispersion

Table II. Particle Size of UA, SDs, and PMs

Product	Particle size (μm)−D_{90}
UA	79.03±27.80
PM001	94.68±34.14
PM002	91.84±32.95
PM003	87.28±31.66
PM004	103.3±35.70
SD001	115.70±39.44
SD002	99.42±36.49
SD003	114.90±38.76
SD004	59.38±21.03

UA ursolic acid, *PM* physical mixture, *SD* solid dispersion

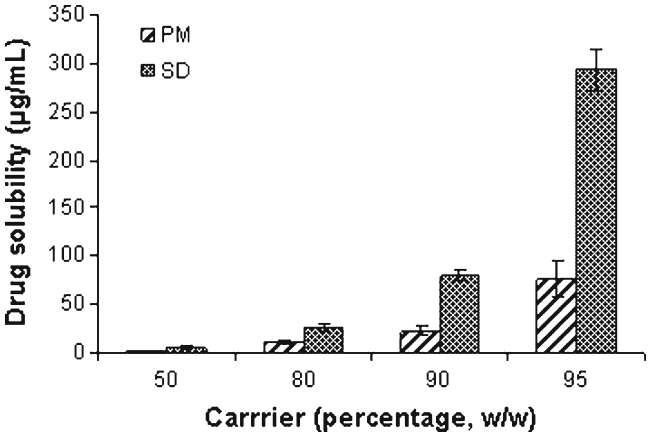

Fig. 6. Determination of the aqueous solubility of UA in PMs and SDs with various ratios of carrier to drug

with the PMs. The highest UA dissolution enhancement was achieved with the formulation containing 95% carrier (SD004), which dissolved approximately 80% after 3 h. The observed behavior was maintained after 6 months of storage for products containing 5% UA.

Cytotoxicity

Cytotoxicity was evaluated for products containing 5% UA, SD004, and PM004. The results presented in Fig. 8 demonstrate that 100% cellular viability was maintained for 8, 32, 128, and 256 µM drug concentrations.

Trypanocidal Activity

In vitro trypanocidal assay results are shown in Table III. The 250-µM UA concentration provoked the highest *T. cruzi* Y strain lysis for both the PM (33.62±1.40) and the SD (48.27 ±4.20). Furthermore, the SD displayed higher trypanocidal activity than the PM, displaying an IC50 of 219.2 and 396.7 µM, respectively

DISCUSSION

There is evidence that UA bioavailability is limited by permeability because its isomer, oleanolic acid, occupies class IV in the Biopharmaceutics Classification System (23). Therefore, drug solubility enhancement and faster dissolution may not be sufficient to increase UA bioavailability. To address to this problem, a formulation containing a penetration enhancer could be developed, which may increase UA cell membrane permeability and thus enhance trypanocidal activity. In previous studies, our group tested SDs containing Poloxamer 407, which is a polymeric surfactant that has been described as a permeability enhancer (24). However, despite the observed enhancement in UA dissolution, Poloxamer 407 in SDs did not improve UA trypanocidal activity, most likely because of the low intrinsic ability of Poloxamer 407 to favor parasite cell entry of the highly lipophilic UA.

In this work, our group studied Gelucire 50/13, which is a member of a different surfactant carrier family that has been described as a penetration enhancer, a characteristic attributed to its surfactant and lipid nature. Lipid surfactants such as Gelucire reportedly cause cell membrane polar defects, thus changing their physical properties and making them more permeable (25,26). SDs prepared with Gelucire, however, are usually sticky and tacky. Thus, silicon dioxide was used as an excipient in the Gelucire-based SD products, as reported by Chauhan and collaborators (9), who studied glibenclamide SDs using Gelucire and silicon dioxide as carriers. In addition to imparting good flow to the powder, silicon dioxide has surface silanol groups that are available for hydrogen bonding that potentially interact with the drug, causing faster dissolution by improving drug particle wettability (27).

Products prepared with 5%, 10%, and 15% (*w*/*w*) silicon dioxide had a sticky consistency and thus could not be milled to produce a dry and flowable powder. Only the SD prepared with 20% (*w*/*w*) Gelucire resulted in a dry and fragile mass that was milled, producing a homogenous drug powder that was then characterized. This is important from an industrial

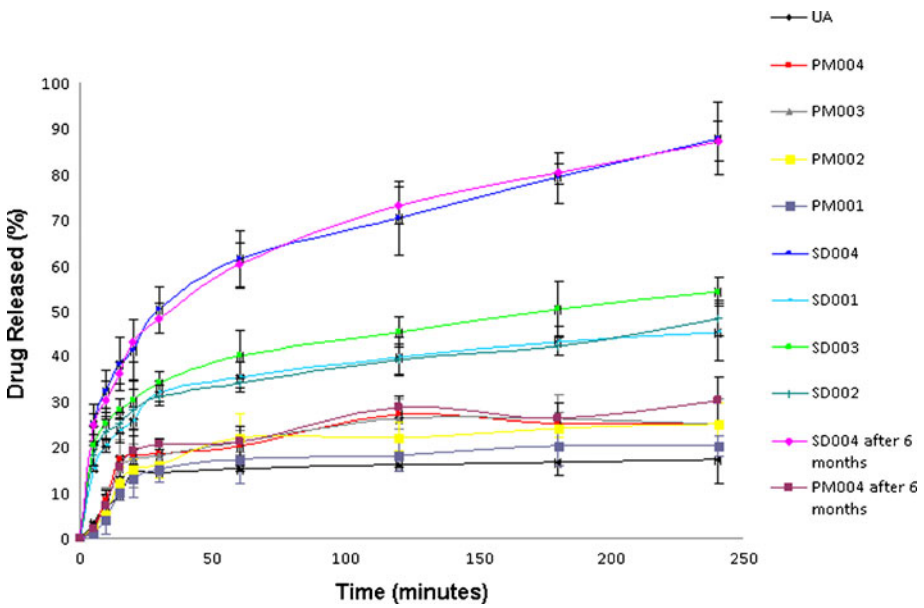

Fig. 7. Dissolution profile of UA as a pure drug, in PMs and in SDs determined in a phosphate-buffered medium containing 1% sodium lauryl sulfate

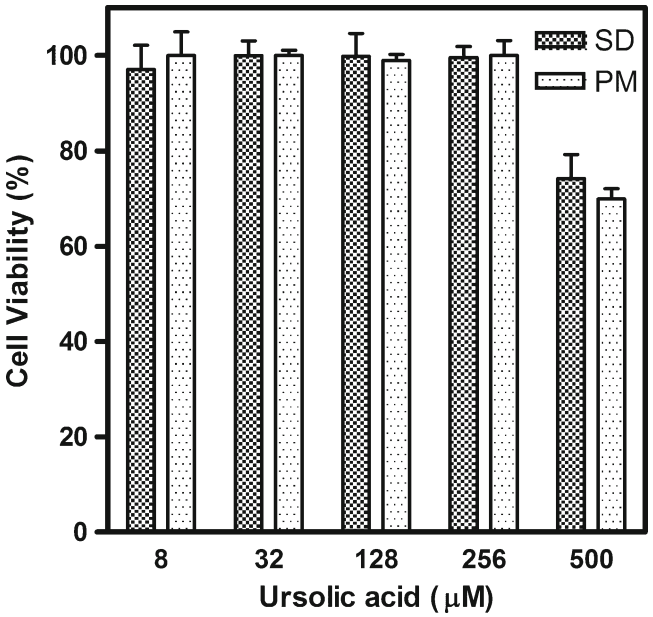

Fig. 8. Cellular viability in percentage of LLC-MK2 fibroblasts after incubation with different concentrations of PM and SD containing 5% UA

perspective because pulverization is one of the most problematic steps during the industrial manufacturing process (28). Moreover, the solvent method employed produced homogenous dry powders in which drug content was between 89.79 and 104.56 (p/p) of the UA amount added to the products (Table I), indicating that the process enabled SD manufacturing with no appreciable losses.

Intermolecular interactions such as hydrogen bonding between the drug and the carrier can be important for enhancing lipophilic drug solubility. As shown in Fig. 1, UA has a carboxyl group that can act as a proton donor or acceptor, thus allowing it to interact with the carboxyl group in Gelucire or the hydroxyl groups in silicon dioxide. Such interactions would be expected to shift or broaden the FTIR peaks corresponding to the participating groups (2). Figure 2 shows that intermolecular interactions took place between the drug and the carriers in the SD, as shown by the progressive broadening of the carbonyl band with increasing Gelucire content, compared with the PM, in which the carbonyl bands remained sharp.

Thermal analyses are important in SD characterization because they provide important information regarding the stability and storage of those systems. Such analyses may also reveal the occurrence of possible incompatibilities between the drug and the excipients or even changes in the solid-state drug characteristics (29). Figure 4 shows the melting points of Gelucire and UA (45°C and 280°C, respectively), which are associated with their endotherms in the DSC analysis. Moreover, it is important to note an exothermic peak for pure UA at approximately 200°C, which is characteristic of a crystallization event and could be associated with a polymorphic conversion with temperature increase. This phenomenon is similar to what has been observed with alprazolam in the paper by De Armas and collaborators (30), who characterized the polymorphisms in this drug through DSC.

Figure 4 shows that DSC experiments were not able to distinguish SDs from PMs. Disappearance of the melting endotherm of the drug in SDs and PMs that contain low drug concentrations (5% or 10%) is evident, which is a commonly observed finding. This phenomenon could be related to either UA conversion from a crystalline to an amorphous structure in SDs, dissolution of the drug in the molten carrier in both SDs and PMs, or a combination of these two events (31). Conversely, in systems containing larger drug amounts (50% or 20%), it is possible to identify the UA melting endotherm because it is present in excess. As a result, the drug either does not solubilize completely in the molten polymer, or is not fully converted to the amorphous form, and the excess drug is deposited as crystals within the polymer matrix.

Hot stage microscopy experiments were conducted to better understand how the drug is dispersed within the carrier, what thermal events are associated with UA heating and to visualize whether the drug dissolves in the molten polymer after heating. After melting the Gelucire, the remaining UA solid content partially dissolved in the molten mass, which may explain the unobserved melting endotherm for the SDs and the PMs containing 10% or 5% of the drug. The exothermic event at 200°C that was observed for UA in the DSC experiments was also visualized by microscopy, which revealed small needle-like crystals growing. A similar finding has already been reported for carbamazepine, which was attributed to polymorph conversion at high temperatures (32). Importantly, this characteristic was preserved in the PMs, but it was not observed for the SDs, which indicates that SD formation altered the solid-state properties of UA. Furthermore, this may indicate that the SD technique changed the drug state from crystalline to amorphous, which did not undergo crystalline conversion at 200°C.

Another important tool for solid dispersion characterization is the X-ray diffraction pattern, which shows the crystalline nature of the systems. Figure 5 reveals that the UA X-ray peaks at 6°, 8°, and 15° are maintained in the PMs with intensities that are directly proportional to the amount of drug in the systems. However, these peaks are broadened and less intense in SDs with higher drug concentrations and almost disappear in the SD containing 5% drug. This observation

Table III. *In Vitro* Trypanocidal Activity of UA in PM and SD Against the Y Strain of *T. cruzi*

	% Lysis±SD/concentration (μM)				
Product	8	32	128	256	IC_{50} (μM)
PM004	0±0	0.43±0.04	34.48±3.10	33.62±1.40	396.7
SD004	3.44±0.31	8.62±0.87	44.82±2.88	48.27±4.20	219.2

PM physical mixture, *SD* solid dispersion, IC_{50} inhibitory concentration

could indicate conversion of UA crystals to an amorphous structure in the SDs. This conversion may have been incomplete because of the presence of small remaining peaks; however, the decrease of the most intense UA peak at 15° is evident in the SDs compared to the PMs. The observed conversion from the crystalline to the amorphous form is commonly found in SDs prepared by solvent methods, and Gelucire has been demonstrated to form SDs with drugs in the amorphous state (7,10).

Figure 6 shows the better solubilization in SDs compared with PMs, which was proportional to the Gelucire content. As a surfactant, Gelucire forms micelles in aqueous media, causing lipophilic compound solubilization (6). Among other factors, the higher solubility values observed for the SDs may be attributed to the conversion of UA from the crystalline to the amorphous state, which may be more soluble because there is no crystal lattice to be broken during dissolution studies, making the process more energetically favorable (33).

The dissolution studies were carried out at sink conditions by incorporating 1% sodium lauryl sulfate in phosphate buffer at pH 6.8, which makes the dissolution experiment more physiologically meaningful because of bile salt presence in the gastrointestinal tract (34,35). From Fig. 7, it is evident that dissolution of pure UA is very low, and it is not greatly modified by formulation as a PM. Conversely, a dramatic enhancement in the UA dissolution rate was observed for the SDs, in which the drug and hydrophilic polymers are in close contact. The products containing larger carrier amounts presented higher dissolution profiles, as expected. Possible mechanisms for the observed solubility improvements were described by Ford (36) and include carrier solubilization effects, aggregation absence, improved wettability, and drug conversion to the amorphous state. Additionally, particle size reduction plays an important role in solubility because of increased contact area. As demonstrated in Table II, the product SD004, which contained 5% drug, has a d_{90} particle size of 59.38 μm, smaller than pure UA.

The SD containing 5% drug, which had the highest dissolution rate, and the PM containing the same drug load were also analyzed after 6 months of room temperature storage. Drug content determination (Table I) demonstrated the chemical stability of UA because the SD maintained 90.03% of the labeled UA content, which was initially 91.16%. Additionally, physical stability was demonstrated through an XRD assay, shown in Fig. 5. The resulting data demonstrated that UA did not revert to the crystalline state, a stability problem commonly present in SDs, which can be avoided by surfactant carriers such as Gelucires (6). Together, these results help to explain the maintenance of the SD dissolution profile after the storage period (Fig. 7).

When investigating compounds with activity against Chagas disease, it is critical to assess their therapeutic potential, as evaluated by trypanocidal activity, and to verify a lack of mammalian cytotoxicity. Thus, cytotoxicity studies using Rhesus monkey kidney epithelial cells (LLC-MK2), a cellular model for toxicity evaluation, were performed and demonstrated that both PM004 and SD004 containing 5% UA are safe at concentrations equivalent to 8, 32, 156, and 256 μM because cellular viability was maintained at approximately 100% (Fig. 8). These products were also evaluated for their trypanocidal activity *in vitro* (Table III), which revealed increased lysis of *T. cruzi* trypomastigote forms, and consequently, lower IC_{50} for SD compared to PM. These results are in accordance with the higher dissolution and solubility achieved with Gelucire-prepared SDs.

Despite enhanced UA dissolution in the SD that contained 95% Gelucire and silicon dioxide, *in vivo* tests are still needed to determine the effects of UA carried by SD in Chagas disease treatment. Pharmacokinetic studies will also need to be developed to investigate whether the SD enhances UA oral bioavailability.

CONCLUSION

The results obtained in this study demonstrated improvements in the solubility and dissolution of the lipophilic drug ursolic acid in solid dispersions compared with physical mixtures, which was maintained after 6 months of room temperature storage. This result could be attributed to improved wettability, micellar solubilization caused by the lipid surfactant Gelucire, conversion of ursolic acid from a crystalline to an amorphous structure, or hydrogen bond formation between the carriers and drug. Taken together, these results may explain the improved *in vitro* trypanocidal activity of ursolic acid in solid dispersion compared to the physical mixture, which were also demonstrated to be safe against mammalian fibroblast cells. Therefore, the results presented in this work are promising for development of a dosage form containing ursolic acid to treat Chagas disease.

ACKNOWLEDGMENTS

The authors would like to thank *Coordenação de Aperfeiçoamento de Pessoal de Nível Superior* and *Conselho Nacional de Desenvolvimento Científico e Tecnológico* for financial support.

REFERENCES

1. Maulvi FA, Dalwadi SJ, Thakkar VT, Soni TG, Gohel MC, Gandhi TR. Improvement of dissolution rate of aceclofenac by solid dispersion technique. Powder Technol. 2001;207:47–54.
2. Verheyen S, Blaton N, Kinget R, Van den Mooter G. Mechanisms of increased dissolution of diazepam and temazepam from polyethylene glycol 6000 solid dispersion. Int J Pharm. 2002;249:45–58.
3. Vasconcelos T, Sarmento B, Costa P. Solid dispersions as strategy to improve oral bioavailability of poor water soluble drugs. Drug Discov Today. 2007;12:1068–75.
4. Goddeeris C, Van Den Mooter G. Free flowing solid dispersions of the anti-HIV drug UC 781 with Poloxamer 407 and a maximum amount of TPGS 1000: investigating the relationship between physicochemical characteristics and dissolution behavior. Eur J Pharm Sci. 2008;35:104–13.
5. Majerik V, Charbit G, Badens E, Howath G, Szokonya L, Bosc N, Teillaud E. Biovailability enhancement of an active substance by supercritical antisolvent precipitation. J Supercrit Fluids. 2007;40:101–10.
6. Karatas A, Yuksel N, Baykara T. Improved solubility and dissolution rate of piroxicam using Gelucire 44/14 and labrasol. Farmaco. 2005;60:777–82.
7. El-Badri M, Fetih G, Fath M. Improvement of solubility and dissolution rate of indomethacin by solid dispersions in Gelucire 50/13 and PEG 4000. Saudi Pharm J. 2009;17:217–25.

8. Vippagunta S, Maul K, Tallavayhala S, Grant D. Solid-state characterization of nifedipine solid dispersions. Int J Pharm. 2002;236:111–23.
9. Chauhan B, Shimpi S, Paradkar A. Preparation and evaluation of glibenclamide-polyglycolized glycerides solid dispersions with silicon dioxide by spray-drying technique. Eur J Pharm Sci. 2005;26:219–30.
10. Fini A, Moyano J, Ginés J, Perez-Martinez J, Rabasco A. Diclofenac salts II. Solid dispersions in PEG6000 and Gelucire 50/13. Eur J Pharm Biopharm. 2005;60:99–111.
11. Fukushima K, Terasaka S, Haraya K, Kodera S, Seki Y, Wada A, Ito Y, Shibata N, Sugioka N, Takada K. Pharmaceutical approach to HIV inhibitor atazanavir for bioavailability enhancement based on solid dispersion system. Biol Pharm Bull. 2007;30:733–8.
12. Liu J. Oleanolic acid and ursolic acid: research prospectives. J Ethnopharmacol. 2005;100:92–4.
13. Li G, Zhang X, You J, Song Y, Sun Z, Xia L, Suo Y. Highly sensitive and selective pre-column derivatization high-performance liquid chromatographic approach for rapid determination of triterpenes oleanolic and ursolic acids and application to Swertia species: optimization of triterpene acids extraction and pre-column derivatization using response surface methodology. Anal Chim Acta. 2011;688:208–18.
14. Takada K, Nakane T, Masuda K, Ishii H. Ursolic acid and oleanolic acid, members of pentacyclic triterpenoids acids, suppress TNF-α-induced E-selectin expression by cultured umbilical vein endothelial cells. Phytomedice. 2010;17:1114–9.
15. Bonaccorsi I, Altieri F, Sciamanna I, Oricchio E, Grillo C, Contartese G, Galati M. Endogenous reverse transcriptase as a mediator of ursolic acid's anti-proliferative and differentiating effects in human cancer cell lines. Cancer Lett. 2008;263:130–9.
16. Saravanan R, Viswanathan P, Pugalendi V. Protective effect of ursolic acid on ethanol-mediated experimental liver damage in rats. Life Sci. 2006;78:713–8.
17. Ferreira DS, Esperandim VR, Toldo MPA, Saraiva J, Cunha WR, Albuquerque S. Trypanocidal activity and acute toxicity assessment of triterpene acids. Parasitol Res. 2010;106:985–9.
18. Saraiva J, Lira AAM, Esperandim VR, Ferreira DF, Ferraudo AS, Bastos JK, Andrade e Silva ML, Gaitani CM, Albuquerque S, Marchetti JM. (−)-Hinokinin-loaded poly(D, L-lactide-co-glycolide) microparticles for Chagas disease. Parasitol Res. 2010;106:703–8.
19. Eloy JO, Oliveira ECV, Marotta-Oliveira SS, Saraiva J, Marchetti JM. Desenvolvimento e validação de um método analítico por CLAE para quantificação de ácido ursólico em dispersões sólidas. Quim Nova. 2012;35:1036–40.
20. Cunha WR, Crevelin EJ, Arantes GM, Crotti AEM, Andrade e Silva ML, Furtado NAJC, Albuquerque S, Ferreira DS. A study of the trypanocidal activity of triterpene acids isolated from *Miconia* species. Phytother Res. 2006;20:274–8.
21. Grael CFF, Vichnewski W, Souza GEP, Lopes JLC, Albuquerque S, Cunha WR. A study of the trypanocidal and analgesic properties from *Lychnophora granmongolense* (Duarte) Semir & Leitão Filho. Phytother Res. 2000;14:203–6.
22. Brener Z. Therapeutic activity an criterion of cure on mice experimentally infected with *Trypanosoma cruzi*. Rev Inst Med Trop Sao Paulo. 1962;4:389–96.
23. Tong HH, Du Z, Wang GN, Chan HM, Chang Q, Lai LC, Chow AH, Zheng Y. Spray freeze drying with polyvinylpyrrolidone and sodium caprate for improved dissolution and oral bioavailability of oleanolic acid, a BCS Class IV compound. Int J Pharm. 2011;404:148–58.
24. Monti D, Burgalassi S, Rossato MS, Albertini B, Passerini N, Rodriguez L, Chetoni P. Poloxamer 407 microspheres for orotransmucosal drug delivery. Part II: *in vitro*/*in vivo* evaluation. Int J Pharm. 2010;400:32–6.
25. Li X, Nie SF, Kong J, Li N, Ju CY, Pan WS. A controlled-release ocular delivery system for ibuprofen based on nanostructured lipid carriers. Int J Pharm. 2008;363:177–82.
26. Liu R, Liu Z, Zhang C, Zhang B. Gelucire 44/14 as a novel absorption enhancer for drugs with different hydrophilicities: *in vitro* and *in vivo* improvement on transcorneal permeation. J Pharm Sci. 2011;100:3186–95.
27. Yassin A, Alenazi F, El-Badry M, Asana I, Barakat N, Alenazi F. Preparation and characterization of spironolactone-loaded gelucire microparticles using spray-drying technique. Drug Dev Ind Pharm. 2009;35:297–304.
28. Newa M, Bhandari K, Li X, Kwon T, Kim J, Yoo B, Woo J, Lyoo W, Yong C, Choi H. Preparation, characterization and *in vivo* evaluation of ibuprofen binary solid dispersions with poloxamer 188. Int J Pharm. 2007;343:228–37.
29. Ramos L, Cavalheiro E. Thermal behavior of loratadine. J Therm Anal Calorim. 2007;87:831–4.
30. De Armas HN, Peeters OM, Mooter GVD, Blaton N. Polymorphism of alprazolam (Xanax): a review of its crystalline phases and identification, crystallographic characterization, and crystal structure of a new polymorph (form III). J Pharm Sci. 2007;96:1114–30.
31. Ali W, Williams AC, Rawlinson CF. Stochiometrically governed molecular interactions in drug: poloxamer solid dispersions. Int J Pharm. 2010;391:162–8.
32. Naima Z, Siro T, Juan-Manual GD, Chantal C, René CJ. Interactions between carbamazepine and polyethylene glycol (PEG) 6000: characterizations of the physical, solid dispersed and eutectic mixtures. Eur J Pharm Sci. 2001;12:395–404.
33. Taylor LS, Zografi G. Spectroscopic characterization of interactions between PVP and indomethacin in amorphous molecular dispersions. Pharm Res. 1997;14:1691–8.
34. Damian F, Blaton N, Naesens L, Balzarini J, Kinget R, Augustijns P, Van Den Mooter G. Physicochemical characterization of solid dispersions of the antiviral agent UC-781 with polyethylene glycol 6000 and Gelucire 44/14. Eur J Pharm Biopharm. 2000;10:311–22.
35. Serajuddin ATM, Sheen PC, Augustine MA. Improved dissolution of a poorly water-soluble drug from solid dispersions in polyethylene: polysorbate 80 mixtures. J Pharm Sci. 1990;79:463–4.
36. Ford JL. The current status of solid dispersions. Pharm Acta Helv. 1986;61:69–88.